# Chemical Wave Driven Convection in Capillary Tubes

by

**Doyle W. Rose**

A thesis submitted in conformity with the requirements

for the degree of Master of Science

Department of Physics

University of Toronto



Unpublished, see also http://mobydick.physics.utoronto.ca

# Abstract

Chemical wave propagation in thin capillary tubes was studied by using the iodate-arsenous acid reaction with a pH indicator. The speed of the reaction front was measured for upwards, downwards, horizontal and inclined front propagation. It is believed that downward propagation gives a front speed which is purely determined by the reaction kinematics. Front speeds greater than this are thought to be assisted by convection. Such greater front speeds were observed for upwards and most inclined propagation. However, fronts propagating horizontally and inclined near the horizontal had front speeds less than the downwards speed. This was unexpected, since theory and previous experiments had shown that the horizontal front speed was greater than the downwards front speed. It is not known if this slow horizontal front speed is a convective effect, or due to some other factor. In addition to the effect of angle, the effect of tube diameter on convection was also studied. Convection for upwards propagation had an onset diameter between 1.90 mm and 2.05 mm. For inclined angles, convection was observed in tubes of all diameters. The front speed increased as the tube diameter was increased, indicating that convection is more vigorous in larger tubes.

# Acknowledgements

I would like to thank my supervisor, Prof. Stephen W. Morris. I would also like to thank the members of the Nonlinear Group at the University of Toronto, Kiam Choo, Zahir Daya, Vatche Deyirmenjian, Malcolm Graham, Tim Molteno, Wayne Tokaruk, for their help and support. I must also extend thanks to the undergraduate laboratories for the use of some of their equipment, as well as the the physics department machine shop for their assistance in the construction of the apparatus used.

# Contents

# List of Figures

# List of Tables

# Chapter 1

# Introduction

## 1.1 General Front Theory

The field of nonlinear and nonequilibrium physics offers a number of interesting and practical subjects for study. One of these is the formation of patterns in physical systems. Of particular interest is the formation of patterns in chemical reactions. These patterns are of interest because they are properties of the physical processes involved in the reaction. As such, they can be used to observe and evaluate the processes that take place. The mixing of chemicals is one such process. The rates at which chemicals mix can play a large role in how quickly and thoroughly an amount of chemicals can be made to react into some desired product. Fluid flow through a mixture of chemicals can enhance the reaction by bringing reactants together at a faster rate. One source of fluid flow is convection, which is the topic of this project. Convection will be studied in a chemical mixture by looking at chemical waves.

Chemical waves are a phenomenon associated with autocatalytic chemical reactions. In an autocatalytic chemical reaction, the reaction produces a catalyst. As diffusion carries this catalyst through the solution, the catalyst comes into contact with unreacted solution. The catalyst causes the unreacted solution to react, producing more catalyst in the process. In this way the reaction propagates through the fluid until all of the reactants have been consumed. This propagation occurs as a chemical wave, or front. The reaction-diffusion mechanisms of these chemical

waves can produce a number of phenomenon, such as spiral waves, chemical chaos and Turing patterns [1].

Convection is a hydrodynamic flow driven by differences in the relative buoyancies of the reacted and unreacted solutions. Hydrodynamic instability, which causes convection, arises from two sources. The first source is the density difference caused by the chemical concentration differences between the reacted and unreacted fluids across a front. This can lead to a situation similar to the classical Rayleigh-Taylor instability, in which two immiscible fluids of different densities are placed one on top of the other with the heavier one on top [2]. The second source is thermal effects. If the temperature difference between the two fluids due to an exothermic reaction is great enough, the resulting density gradients due to thermal expansion can result in a Rayleigh-Bénard-like instability. In this instability, convection in a fluid layer is driven by heating from below [2]. It will be shown later that neither of these two sources of convection drive chemical waves.

In this study, the iodate-arsenous acid reaction was used. In this reaction, the unreacted solution is converted into a less dense reacted solution at a sharp moving front. The iodate oxidation of arsenous acid is described in terms of two component processes. These are the Dushman reaction [3]

$$IO_3^- + 5I^- + 6H^+ = 3I_2 + 3H_20 \tag{1.1}$$

and the Roebuck reaction [3]

$$H_3As0_3 + I_2 + H_20 = H_3As0_4 + 2I^- + 2H^+. \tag{1.2}$$

When arsenous acid is in stoichiometric excess the net reaction is

$$IO_3^- + 3H_3AsO_3 = I^- + 3H_3AsO_4. \tag{1.3}$$

When iodate (the autocatalyst) is in stoichiometric excess, the net reaction is

$$2IO_3^- + 5H_3AsO_3 + 2H^+ = I_2 + 5H_3AsO_4 + H_2O. \tag{1.4}$$

When neither reactant is in stoichiometric excess, that is

$$\frac{5}{2}[IO_3^-]_0 < [As(III)]_0 < 3[IO_3^-]_0$$

(where $[\cdots]_0$ denotes the initial chemical concentration), the net reaction is a linear combination of Equations 1.3 and 1.4 [3].

The reaction is slightly exothermic, so that only a small amount of heat is produced. The length scale over which temperature variations occur is much larger than the volume around the reaction front. Thus the produced heat diffuses away from the front, mainly into the unreacted fluid [2]. Consequently the fluid in the vicinity of the front, both reacted and unreacted, can be considered to have a uniform temperature which by convention is taken to be the higher temperature of the reacted solution. Hence for this reaction, the difference in density between the reacted and unreacted fluids is due only to differences in their compositions [1].

As the front propagates through the solution, there is no surface tension between the front and the tube walls. This is because the propagation of the front is merely the diffusion of the autocatalyst through the solution. Thus, meniscus effects do not influence the front.

If the iodate-arsenous acid reaction propagates vertically upwards in a capillary tube then the more dense unreacted solution is on top of the less dense reacted solution. This configuration is potentially unstable. However, the reaction-diffusion mechanism that drives the front is dependent on the front curvature. This dependence is given by the "eikonal" relation for the front speed

$$C = C_0 + D_c\kappa \tag{1.5}$$

where $C$ is the normal velocity of the front, $C_0$ is the convectionless (flat) front speed,

$D_c$ is the molecular diffusivity of the catalyst, and $\kappa$ is the curvature of the front, taken to be positive when the center of curvature is in the unreacted fluid. Should the front begin to deviate from being flat, the eikonal relation provides a stability mechanism for the front. At peaks, negative curvature lowers the front speed, while in valleys, positive curvature increases the front speed, thus flattening the front [2]. The front is therefore stable to small-wavelength, small-amplitude perturbations. As tube size increases, buoyancy effects, which form the hills and valleys, become stronger. This leads to larger hills and valleys, which eventually become too large for the stabilizing mechanism to suppress. Thus, in tubes of larger diameters, the interaction between the stabilizing (reaction-diffusion) and destabilizing (buoyancy) mechanisms leads to hydrodynamic instability and convection [4].

The form of convection seen in the iodate-arsenous acid reaction is different from Rayleigh-Taylor and Rayleigh-Bénard convection. A curved front with travelling convective rolls distinguishes the iodate-arsenous acid reaction from the Rayleigh-Taylor problem. In the Rayleigh-Taylor problem, the surface tension between the two immiscible fluids provides the stabilizing mechanism. For the iodate-arsenous acid reaction, the stability mechanism is provided by reaction-diffusion. This mechanism is not possible in the Rayleigh-Taylor problem because the two fluids are immiscible. The iodate-arsenous acid reaction differs from Rayleigh-Bénard convection because the convective roll travels with constant speed and because the instability is driven by a nonlinear chemical composition profile and not by a linear temperature profile [4].

## 1.2 Convection and Front Speed

Convection was studied by observing how the iodate-arsenous acid reaction front behaves as it propagates through thin capillary tubes. In a downward propagating front the less dense reacted solution is on top of the more dense, unreacted solution. This configuration is stable and no convection occurs. The front is flat propagates at a constant speed determined by the coupling of reaction and diffusion. The descending

front therefore provides the speed for the pure reaction-diffusion wave. A speed greater than that of the descending front must be the result of convection [3].

If the propagation is upwards then the more dense unreacted solution is on top of the less dense reacted solution. This configuration is unstable and may result in convection. If the tube is wide enough, buoyancy effects will be strong enough to destabilize the flat front provided by the reaction-diffusion mechanism, which was described in the previous section.

If the tube is horizontal, there will always be convection. This effect is qualitatively explained by Pojman et. al. [3]. They describe the horizontal case as being analogous to a system with fluid between two vertical, differentially heated plates. Such a configuration is always unstable, so there should not be a critical diameter for the onset of convection.

If the tube is inclined away from the horizontal, more interesting effects are seen. Convection is observed at all inclined angles, even when the tube is too small for convection due to upwards front propagation to take place. In addition, there is an angle between horizontal and upwards propagation at which the front speed is a maximum. A qualitative explanation for this effect was provided by Nagypál, Bazsa and Epstein [5]. The horizontal cross section of an inclined tube is larger than the perpendicular cross section. Thus, convection can appear as it does in wider tubes. As the cross section increases, the front speed increases as it does for increasing tube diameters. At the same time, the convective roll travels shorter distances before reaching the inclined walls of the tube. This inhibits motion in the vertical direction, slowing the front. The competition between these two effects yields a maximum front speed between the horizontal and vertical directions. This effect has not been well studied previously, and will be examined in this work.

## 1.3 Models

Fronts observed in the iodate-arsenous acid reaction can be modelled using a one-variable reaction-diffusion equation coupled with the hydrodynamic equations of mo-

tion [1, 2, 4, 6, 7]. As mentioned previously, a heat diffusion equation is not necessary, since the length scale over which temperature variations occur is much larger than the size of the convective rolls [6]. The heat diffuses away from the front and the temperature in the vicinity of the front can be considered to be constant.

The equations governing the hydrodynamics are

$$\frac{\partial \mathbf{V}}{\partial t} + (\mathbf{V} \cdot \nabla)\mathbf{V} = -\frac{1}{\rho}\nabla P_r + \nu \nabla^2 \mathbf{V}, \tag{1.6}$$

$$\nabla \cdot \mathbf{V} = 0. \tag{1.7}$$

Here $\mathbf{V}$ is the fluid velocity, $\rho$ is the density of the fluid, $\nu$ is the kinematic viscosity and $P_r$ is the reduced pressure, given by $P_r = P + \rho g \hat{z}$. [7].

The reaction-diffusion equation is given by

$$\frac{\partial c}{\partial t} + \mathbf{V} \cdot \nabla c = D\nabla^2 c + f(c) \tag{1.8}$$

where $c$ is the iodide concentration $[I^-]$, $D$ is the molecular diffusivity and $f(c)$ is the reaction term. For the iodate-arsenous acid reaction, the reaction term is the third order polynomial

$$f(c) = -\alpha c(c - c_2)(c - c_3) \tag{1.9}$$

where $c_2$ is the initial concentration of iodide $[IO_3^-]_0$, $c_3 = -k_a/k_b$ is the ratio of two reaction rate constants, and $\alpha = k_b[H^+]^2$ [8].

This reaction-diffusion theory assumes that the front has a finite thickness. From experimental observations, the reaction front has been calculated to have a thickness of about 70$\mu$m [2]. This is much less than the other length scales involved in the reaction, such as the length scale for temperature variations (5 mm) and tube diameter (2 mm) [2]. Hence the reaction front can be approximated as a thin boundary between the two fluids [7]. In such a thin-front model, the front has zero thickness and the pressures and velocities of the reacted and unreacted solutions are related by discontinuities across the front. The reaction-diffusion equation is now be replaced with the eikonal relation, given by Equation 1.5 [7].

Standard boundary conditions for these models are no-slip and no-normal-flow at the cylinder walls.

If we transform the hydrodynamic and reaction-diffusion equations (Equations 1.6-1.8) into a dimensionless form, we find that there is only one dimensionless driving parameter that determines the convective stability of the front. This parameter is denoted $S$, and is discussed in detail in the next section.

### 1.3.1 Driving Parameter

The dimensionless driving parameter $S$ measures the strength of buoyancy effects, which tend to destabilize a flat front in favour of convection, relative to curvature effects, which tend to flatten the front [1]. The parameter is

$$S = \frac{\delta g a^3}{\nu D}.$$

The quantity $\delta = (\rho_u - \rho_r)/\rho_r$ is the fractional density difference between the reacted ($\rho_r$) and unreacted ($\rho_u$) solutions. The quantity $g$ is the acceleration of gravity, $a$ is the tube radius, $\nu$ is the kinematic viscosity and $D$ is the molecular diffusivity of the catalyst.

The chemical concentrations are usually small, and $\delta$ is typically on the order of $10^{-4}$. This change is very difficult to measure due to a number of factors, such as the fact that the magnitude of the change is on the order of the thermal expansion of the apparatus. Such a measurement was not attempted in this work. The differences in $\nu$ and $D$ between the reacted and unreacted solutions are negligible. When making calculations, these last two quantities are assumed to be equal to the corresponding values for water [6].

Linear stability calculations using this theory [1, 6] predicted that for upwards propagation, convection will occur for $S > S_c = 87.9$. This convection will be nonaxisymmetric. That is, reacted fluid will rise on one side of the tube and unreacted fluid will fall on the other. If $S$ is further increased, axisymmetric convection will occur for $S > S_{c_2} = 370.2$. In this case, reacted fluid rises in the center of the tube and

unreacted fluid falls down the sides. These values of $S_c$ are universal, independent of tube diameter and fluid parameters [1]. A more thorough discussion of what is meant by axisymmetric and nonaxisymmetric convection follows in Section 1.4. Horizontal convection is always nonaxisymmetric [3].

We see that the stability of the front depends on the cube of the radius of the capillary tube it is propagating in. The stability also depends on the chemistry involved. Specifically, it depends on the densities of the reacted and unreacted fluids, as expected, as well as $D$ and $\nu$. We should note that while the critical values for $S$ are universal, $S$ itself depends on radius, density and other factors. If one factor is changed, then the others must also change to stay at the same $S$. For example, if the density difference is lowered, the front will require a larger tube diameter in order to convect.

In order to predict the onset radius, it will be necessary to determine a value for $\delta$. Since $\delta$ was not measured in the experiment, a value for it must be taken from the literature. The experiment by Mike Carey [9] used the same reactant concentrations and indicator that were used in this experiment. Carey determined $\delta$ to be $4 \times 10^{-5}$. This value gives a predicted onset diameter of $(1.49 \pm 0.07)$ mm.

The dependence of the front on tube radius has been studied extensively and verified by Vasquez *et. al.* [4], Pojman *et. al.* [3] and Masere *et. al.* [6]). Dependence on chemical density has been studied to a lesser degree. This dependence is verified by measurements of front speed as a function of concentration done by Pojman *et. al.* [3] and Masere *et. al.* [6]. Dependence of the front speed on angle has not been done for the iodate-arsenous acid reaction. This will be studied in this work.

## 1.4 Modes of Convection

According to theory, downward propagating fronts are convectionless and hence flat. Upwards propagating fronts have more interesting shapes, as a result of convection. Two forms of convection are seen in upwards propagation. These are called axisymmetric and nonaxisymmetric convection. Nonaxisymmetric convection occurs at the

onset of convection ($S_c$=87.9), while axisymmetric convection occurs for higher $S$, and therefore larger tube diameters.

Nonaxisymmetric convection is illustrated in Figure 1.1a. It consists of a single convective roll confined to the vicinity of the reaction front, with regions of rising and falling fluid separated by a vertical nodal plane through the cylinder axis [1]. This produces an "S" shape. Axisymmetric convection is illustrated in Figure 1.1b. In this case, the fluid rises in the center of the tube and descends along the sides. This results in a parabolic or "donut" front shape [3]. The transition between the two modes of convection is not well understood.

In the case of horizontal propagation one gets nonaxisymmetric fluid flow. This is shown in Figure 1.2 for a horizontal front propagating from left to right [3]. The result is a slanted front, in which the lighter, reacted fluid flows over the heavier, reacted fluid. There is little theory available for the shape of a front propagating away from the horizontal and vertical directions. For $S$ below the critical value for axisymmetric convection, the front at an inclined angle would probably be nonaxisymmetric. If upwards propagation is axisymmetric, an inclined front would probably be a mixture of the two modes. This is only a hypothesis, based on the fact that horizontal propagation is always nonaxisymmetric, and inclined propagation is a mixture of horizontal and vertical propagation.

## 1.5 Review of Previous Experimental Results

Experiments involving the propagation of the iodate-arsenous acid reaction in capillary tubes were carried out by Pojman, Epstein, McManus and Showalter [3]. They looked at the propagation of the front in the vertical (upwards and downwards) and horizontal directions. They also examined the effect of chemical concentrations and measured the enthalpy of the reaction.

The experiments were carried out in water-jacketed glass capillary tubes that were 25.0 cm long with various inner radii. The temperature was held constant at $(25.0 \pm 0.1)$°C. The arsenous acid solution was made from $NaAsO_2$ and $H_2SO_4$ in a

Figure 1.1: Nonaxisymmetric (left) and Axisymmetric (right) Convection for Upwards Propagation

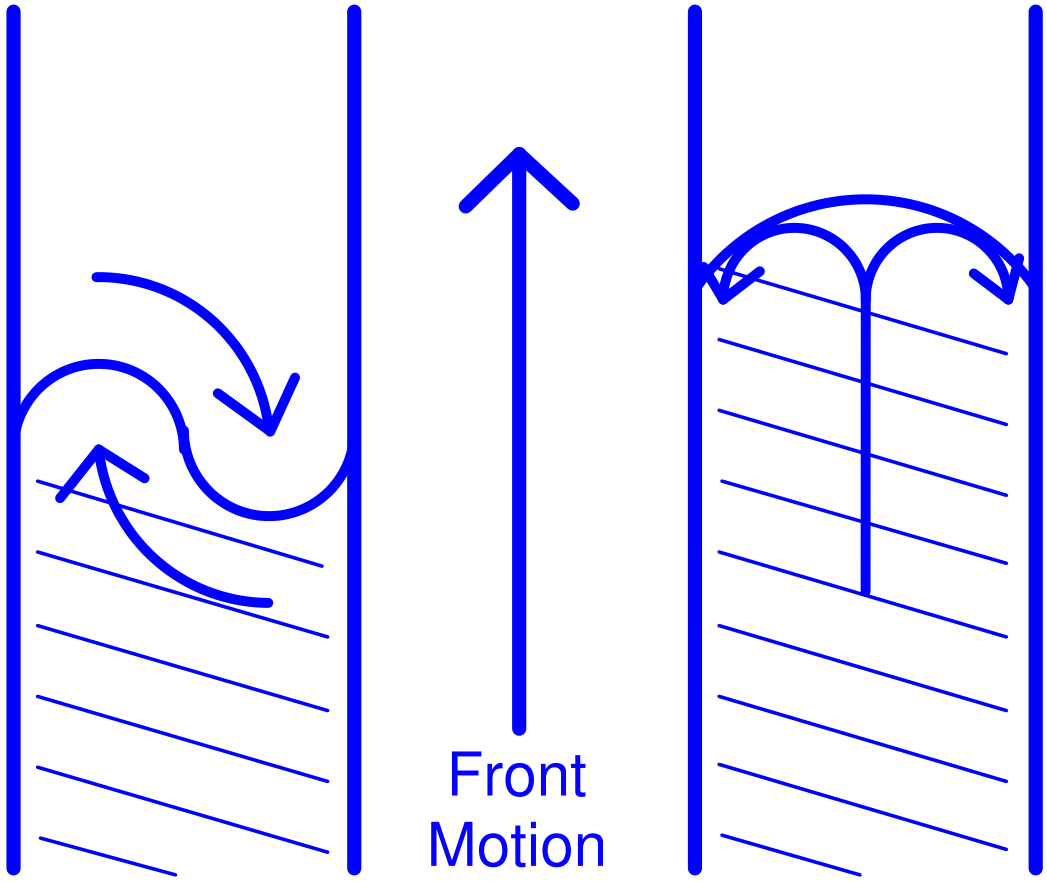


Figure 1.2: Nonaxisymmetric Convection for Left to Right Horizontal Propagation

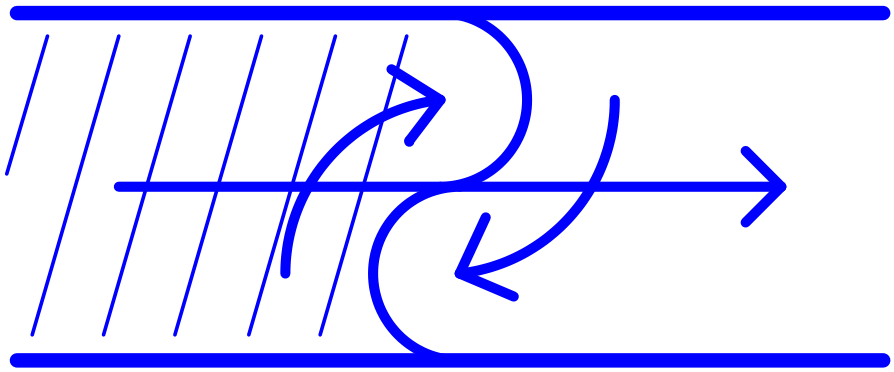

1:1 mole ratio. Waves were initiated at platinum electrodes in each end of the tube.

Pojman *et.al.* propagated fronts in three capillary tubes with diameters 0.96 mm, 1.78 mm and 2.4 mm. For downwards propagation, they found that the front speeds in the three tubes were the same to within the experimental error. These fronts were flat and perpendicular to the direction of propagation. Fronts propagating in the horizontal and upwards directions showed different results. For the 0.96 mm tube, the speed of the upwards propagating front was the same as that for the downwards propagating front. For the other two tubes, the upwards front speed was much greater than the downwards front speed. These faster upwards fronts had a parabolic shape. Horizontal front speeds were much greater than downwards front speeds in all three tubes. These fronts were slanted approximately 45° towards the direction of propagation. When front speed increases were observed, the magnitude of the increase increased with the size of the tube.

Front speed was also found to depend on the concentrations of the reactants. The front speeds increased steadily as the $KIO_3$ concentration was increased from about 3 mM (excess arsenous acid) to 10 mM (excess iodate). When the $H_3AsO_3$ concentration was varied, the results were slightly different. The front speeds increased rapidly as the $H_3AsO_3$ concentration was increased in the initial excess iodate region. When arsenous acid became excessive, the front speeds still increased as a function of concentration, but at a lesser rate.

A temperature rise of 0.3° was measured in 50.0 ml of reaction solution with arsenous acid in excess. This corresponds to an enthalpy of reaction of $\Delta H° = -334 kJ/mol$. When iodate was in excess the enthalpy of reaction was $\Delta H° = -606 kJ/mol$.

Further experimental work was carried out by Masere, Vasquez, Edwards, Wilder and Showalter [6]. Their study looked at propagation in the upwards and downwards directions only.

The experiments were carried out in water-jacketed capillary tubes at temperature $(25.0 \pm 0.1)°C$. The waves were triggered electrochemically using a platinum electrode. The front position as a function of time was measured visually using a millimetre scale

attached to the tube. A digital imaging system was also used.

Experiments were carried out in capillary tubes of different diameters using iodate-arsenous acid solutions of the same composition. It was found that for tubes with internal diameter equal to or less than 1.1 mm, the speed of ascending fronts was the same as the speed of descending fronts. These fronts were flat. For tubes of inner diameter 1.4 mm and larger, the speed of the ascending fronts was higher than the speed of the descending fronts. Further, the ascending front speed increased as the tube diameter increased, while the descending front speed was independent of inner diameter. For tube diameters of 1.4 mm and 1.6 mm, nonaxisymmetric convection was seen. Axisymmetric convection was seen for tube diameters of 2.3 mm and greater.

Experiments were also carried out in the 1.4 mm tube in which the iodate concentration was varied. It was found that downwards front speeds varied linearly with the iodate concentration. This agreed with reaction-diffusion theory. Ascending front speeds were greater than descending front speeds. The difference between the two increased as the iodate concentration increased. All of the ascending fronts were non-axisymmetric. Overall, the effect of changing the iodate concentration had a smaller effect than changing the tube diameter.

These experiments confirmed that nonaxisymmetric fronts are seen near the onset of convection, and that there is no convection in ascending fronts for values of $S$ below the critical value. This critical value for $S$ was determined experimentally. By changing the tube diameter, it was found that $S_c = 77 \pm 21$, which agreed with the theoretical value of 87.9. varying the iodate concentration gave $S_c = 70 \pm 16$, which was slightly below the theoretical value.

Vasquez, Wilder and Edwards did some further work with Littley [4]. Their experiments were used to test the validity of a model which consisted of coupling hydrodynamics with a reaction-diffusion equation. It was found that the theoretical predictions agreed with the experimental observations. They also raised other possible topics for investigation. Among these was the effect tilting the capillary tube would have on the front speed.

Work on chemical reaction fronts has also been done on other chemical reactions.

Nagypàl, Bazsa and Epstein [5] looked at the propagation of the chlorite-thiosulfate reaction in thin tubes. This reaction differs from the iodate-arsenous acid reaction in that this reaction is highly exothermic. Temperature changes as high as 10°C have been observed. The heat produced drives convection along with the density difference.

The experiments were carried out in plastic tubes fixed to a wooden board that could be rotated to a desired angle. The reaction was initiated with a drop of acid in one end of the tube. The experiments were carried out at room temperature ($21.5 \pm 0.5$°C) in an air-conditioned laboratory.

The results from their experiments are similar to what was found in the iodate-arsenous acid reaction. In tubes with large inner diameters, the speed of upward propagating fronts was much greater than that for downward propagating fronts. In tubes with small inner diameter, the front speed was the same for upwards and downwards propagation.

The effect of tilting the tubes was also examined. They found that for tubes thick enough to convect, the maximum front speed velocity occurred between 40° and 60° from the horizontal. At 60° to 90°, the upward component of the wave velocity was greater than the velocity of the upward vertical wave.

Experiments were also carried out to determine the effect of heat conduction with the surrounding medium. It was found that such heat conduction did have a large effect.

## 1.6 Purpose

The purpose of this work was to study the relation between the capillary tube diameter, the angle at which the tube is tilted, and the speed of the front. The iodate-arsenous acid reaction (with an added chemical indicator) was observed as it propagated along a capillary tube. The magnitude to which convection affected fronts propagating vertically upwards and horizontally was studied. The onset diameter for convection was determined, and an attempt was made to locate the transition between nonaxisymmetric and axisymmetric convection. In addition, a previously

unstudied effect was investigated, as suggested in [4]. It is predicted from numerical models [10] that for a given capillary tube diameter, there will be an angle of inclination at which the front speed will be a maximum. Further, this angle should be unique for each diameter, and approach 180° as the tube diameter increases. This hypothesis was tested.

# Chapter 2

# Experimental Method

## 2.1 Chemicals

The chemical reaction used in this project was the iodate-arsenous acid reaction. This reaction is of interest due to several important properties it possesses. One property is the density difference between the unreacted and reacted solutions, which drives convection. Another property is the autocatalytic nature of the reaction. In a capillary tube, the reaction if triggered in one end of the tube will propagate to the other end of the tube without any further assistance from the experimentalist.

To observe the front another property of the reaction was used. There is a significant difference in pH between the reacted and unreacted solutions. A pH indicator, Congo Red dye, is used to distinguish the front. The dye is red for pH above about 5.2 [9] and turns blue when the pH drops below this. Hence the unreacted solution, whose pH was greater than 6, appeared red, while the reacted solution, with a much lower pH, appeared blue.

The reaction could be triggered by using one of several methods. One method is to put a voltage across a part of the solution. The reaction would be triggered on the positive electrode. This method worked well in petri dishes, but not in capillary tubes. It was difficult to insert wires into the ends of the tubes. If the wires were inserted successfully, there was no guarantee that the voltage would trigger the reaction. Success in triggering a reaction depended on the wire used (only platinum

wires worked in capillary tubes) and the surface area of the positive electrode. A large surface area was available in the petri dishes, but not in the capillary tubes.

A second triggering method took advantage of the fact that the reaction starts spontaneously at low pH. This method, which was used in the experiment, involved injecting a drop of concentrated HCl through a syringe into the end of the capillary tubes. The acid was, with two exceptions, always successful in triggering a reaction. However, it was not possible to control the amount of acid injected with total accuracy. The syringe was too large to accurately measure the size of the injection, which was much less than a millilitre. Thus, the initial conditions for different reaction fronts were not identical. Also, the acid may have reacted with the indicator, creating pieces of brown-black deposits which were visible in the tubes. It is presumed that the acid did not diffuse through the solution at a rate quicker than the front.

### 2.1.1 Preparation of Reactants

The first step was to create a supply of stock reactants. According to data from Kolodner [11], the stock solutions should be made with the following approximate concentrations

- 0.1 M $As_2O_3$
- 0.1 M $KIO_3$
- 0.001 M Congo Red Dye.

From these stock solutions the iodate-arsenous acid solution is made. The concentrations of the reactants in this solution, again according from Kolodner [11], should be approximately 0.0025 M.

#### Preparation of Stock Solutions

The stock $KIO_3$ solution was prepared in a 2 liter flask that had been rinsed with distilled water. The flask was filled with $(1000 \pm 5)$ ml of distilled water. To the distilled water was added $(21.400 \pm 0.0005)$ grams of $KIO_3$ powder. The contents of

the flask were thoroughly stirred. This gave a stock solution with molarity ($0.1000 \pm 0.0005$) M.

The Congo Red stock solution was prepared in a similar manner in a 500 ml flask. ($200 \pm 1$) ml of distilled water and ($0.140 \pm 0.001$) grams of Congo Red powder gave a stock solution with molarity $(1.005 \pm 0.009) \times 10^{-3}$ M.

The $As_2O_3$ solution was more difficult to prepare. Another 2 litre flask was filled with ($1000 \pm 5$) ml of distilled water. To this was added ($47 \pm 1$) ml of concentrated (1N) KOH. The addition of base was necessary since $As_2O_3$ does not dissolve in neutral water. To this solution was added ($19.878 \pm 0.0005$) grams of $As_2O_3$ powder. The solution was stirred overnight. The next morning, ($47 \pm 1$) ml of concentrated (1N) HCl was added to the flask to restore the pH.

Once the stirring was completed it was noted that not all of the $As_2O_3$ powder had dissolved. It was necessary to filter the solution. The solution was poured through two dry coffee filters. The filtration resulted in the filters becoming soaked with the $As_2O_3$ solution. Since only the dry weight of the filters was known, it was not possible to get an accurate measure of how much $As_2O_3$ powder had not dissolved. Assuming that about one gram of $As_2O_3$ powder did not dissolve, which is probably a bit of an over-estimate, gives a molarity of ($0.09 \pm 0.01$) M.

### Preparation of Working Solution

To prepare the working solution, ($50.0 \pm 0.2$) ml of the stock $KIO_3$ solution and ($950 \pm 2$) ml of distilled water were put into a 1 litre beaker and stirred. Similarly, ($57.0 \pm 0.2$) ml of stock $As_2O_3$ solution and ($943 \pm 2$) ml of distilled water were transferred to a 2 litre flask and stirred. Then ($20.0 \pm 0.2$) ml of stock Congo Red dye was put into the flask. The diluted $KIO_3$ solution was then poured into the flask, and the working solution was stirred. The solution was clear with a dark red color. The molarities of the reactants were ($0.00247 \pm 0.00002$) M for $KIO_3$ and ($0.0025 \pm 0.0003$) M for $As_2O_3$. The concentration of the Congo Red dye was $(1.0 \pm 0.1) \times 10^{-6}$ M. The pH of this solution was found to be $6.75 \pm 0.01$.

A sample of this solution (about 50 to 60 ml) was removed and tested in the

apparatus (see following sections). The indicator colors were so faint that the front could not be clearly distinguished in the travelling microscope. To solve this problem an additional amount of the stock Congo Red dye, $(54.5 \pm 0.2)$ ml, was added to the flask. This darkened the solution sufficiently so that the front could be seen in the travelling microscope. The new reactant concentrations were $(0.00247 \pm 0.00004)$ M for $KIO_3$ and $(0.0025 \pm 0.0003)$ M for $As_2O_3$. The concentration of the Congo Red dye was $(3.71 \pm 0.07) \times 10^{-5}$ M.

The working solution was stored in a 2 litre flask that was kept capped to prevent evaporation. When the apparatus required new solution, a small amount of solution was poured from the flask into a jar that had been cleaned and rinsed with distilled water. The solution in the jar was then transferred by syringe to the apparatus. In this way the stock working solution was kept clear of contaminants.

## 2.2 Apparatus

The apparatus used consisted of a few simple items. The main apparatus was eight capillary tubes of various inner diameters which were mounted on a board. A travelling microscope was also used for part of the experiment.

### 2.2.1 Capillary Tubes

For this experiment, eight capillary tubes of different internal diameters were used. The tubes were of stock diameters, so the choice of inner diameters was limited. As well, the tubes were not of uniform length, but ranged from about 48 cm to 135 cm in length.

To fill the tubes with the working solution a syringe was used to inject the solution into the tubes. Once the tubes were filled the ends were capped and sealed. The ends were capped with 1 to 2 inch lengths of tygon or rubber tubing. The caps were then pinched shut with finger clamps.

A vernier calipers was used to verify that the eight tubes all had different diameters, since it was sometimes difficult to verify the differences by sight. However, the

calipers were not trusted to give an accurate measurement of the inner diameters. To determine the inner diameters, a different method was used. The lengths of the eight tubes were measured. Then each tube, with its caps and clamps, was weighted. The tubes were then filled with distilled water, capped and reweighed. The difference in the two weights was the weight of the water. Given the water temperature (which was measured with a thermometer) and an estimate of the atmospheric pressure, the density of the water was calculated. With the density known, the diameters of the tubes were calculated. The results are given in Table 2.2.1.

Table 2.1: Inner Diameters, Length and Wall Types for the 8 Capillary Tubes.

| Tube | Diameter | Length | Wall Type |
|---|---|---|---|
| A | $(2.781 \pm 0.006)$ mm | $(90.94 \pm 0.03)$ cm | Thick |
| B | $(2.559 \pm 0.006)$ mm | $(122.4 \pm 0.1)$ cm | Thick |
| C | $(2.417 \pm 0.006)$ mm | $(122.1 \pm 0.1)^*$ cm | Thin |
| D | $(2.249 \pm 0.006)$ mm | $(135.2 \pm 0.1)$ cm | Thick |
| E | $(2.05 \pm 0.01)$ mm | $(91.00 \pm 0.07)$ cm | Thick |
| F | $(1.90 \pm 0.02)$ mm | $(48.3 \pm 0.1)$ cm | Thick |
| G | $(1.80 \pm 0.01)$ mm | $(77.65 \pm 0.07)$ cm | Thick |
| H | $(1.53 \pm 0.01)$ mm | $(91.55 \pm 0.07)$ cm | Thick |

*Original length used in calculation. The final length, after several breaks, was $(73.6 \pm 0.1)$ cm.

This method provided the average diameter. There was no guarantee that the tubes were perfectly uniform in diameter. The possibilities of nonuniformities is discussed in Section 2.4.

Seven of the tubes were thick walled. These tubes had thick glass walls which were several times larger than the inner hole. These tubes were sturdy and were easy to work with. The eighth tube was thin walled. The glass wall of this tube was thinner than the diameter of the inner hole. This tube was fragile and more difficult to work with. During the course of the experiment, the ends of this tube broke off several times, resulting in a decrease in the tube length over time. As well, the thinner wall may have allowed for the solution to be in greater thermal contact with the lab environment than the thick walled tubes. Thus, the solution in the thin walled tube

would be more greatly influenced by changes in room temperature.

### 2.2.2 Tube Mounting

The capillary tubes were mounted to a plywood board that was hung on a dexion frame. The board was hung on the dexion by a screw in the board's centre. The board could be rotated around this screw to any desired angle. Once the proper angle was reached, a clamp was used to hold the board in place.

A diagram of the apparatus appears in Figure 2.2.2. The capillary tubes were mounted to the board parallel to its length and were held in place by small plastic clamps that were screwed into the board at intervals of about 3 cm along its width. The two shortest tubes were placed in the centre slot on either side of the centre screw. Thus eight tubes could be mounted simultaneously.

When the travelling microscope was used, only one tube was mounted. This was mounted to one side of the centre screw. On the other side a metal beam running the length of the board was mounted. The travelling microscope was mounted to this beam through the use of special mounts that were constructed for and screwed into its base. The beam and tube were placed so that the tube would be in the microscope's sight. This configuration is also shown in Figure 2.2.2.

A sheet of polar plot graph paper was used to determine the angle of the board with respect to vertical. the centre of the paper was cut out and the paper was taped to the board so that the 0° to 180° line was parallel to the tubes. The board was rotated to approximately the desired angle. A bob was hung from the centre screw, and the board was rotated until the bob lined up with the desired angle. The angle could be determined to within one half of a degree.

## 2.3 Front Speed Measurement and Calculation

The front speed was quite slow, on the order of 2 cm/hour. To determine these speeds, two different methods were used. For both methods, the front was observed over a set period of time. This length of time was chosen to be appropriate for the

Figure 2.1: Apparatus For the Gatling and Travelling Microscope Methods

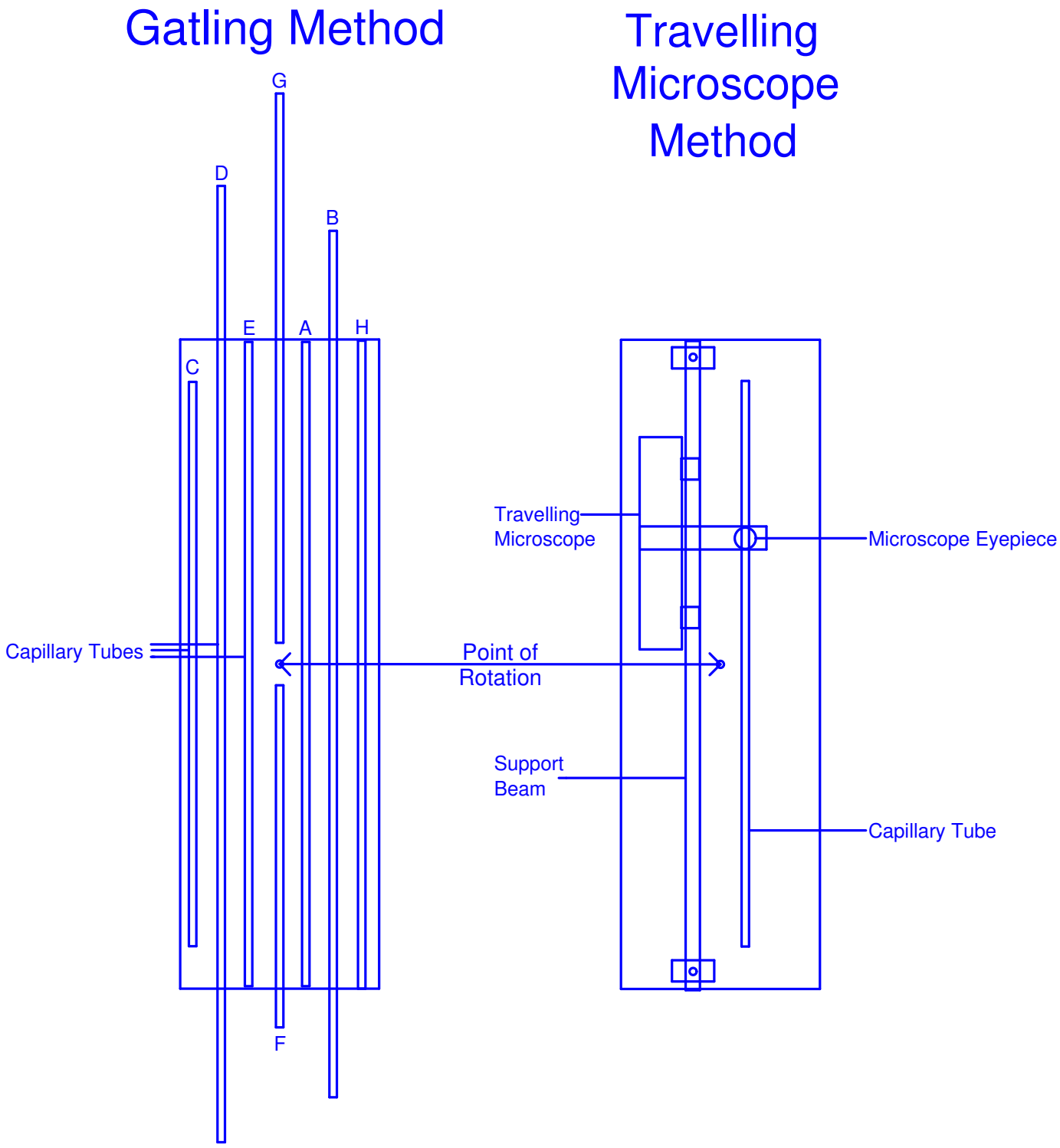

method used. For each method, at semi-regular intervals the position of the front would be recorded. This data for position as a function of time was then entered into a computer program which used a least-squares fitting routine to calculate the front speed.

### 2.3.1 Travelling Microscope Method

The travelling microscope was used to measure the front speed in tubes A, E and G (see table 2.2.1). Tube G was chosen because it was too narrow for convection to occur, tube A was chosen because it was wide and convection could easily occur, and tube E was chosen because its diameter was close to the critical diameter.

The board was rotated to the desired angle and clamped into position. Once the board was at the correct angle the microscope was attached to the beam. The microscope was moved along the beam until the front in the capillary tube could be seen in the microscope. A clamp was then used to secure the microscope at that position, and the initial position and stopwatch time were recorded. At five minute intervals, the microscope would be adjusted to catch up with the front, and the position and time would be recorded. In this way, 10 position/time data points were taken for a given angle. Once this procedure was completed the microscope was removed from the board, which was rotated to a new angle so that the procedure could be repeated. It was found that at most 10 angles could be measured from a single tube of solution. Once the front had reached the end of the tube, the tube was emptied, rinsed with distilled water, dried and refilled with unreacted solution.

For the wide and narrow tubes, the angles measured covered the range from 0° to 180° in steps of 15°. Fronts moving straight downwards were defined to be 0°. These angles were not measured sequentially. Instead, the choice of angle to be measured was varied in a pseudo-random fashion. This was done to minimize the possibility of systematic errors.

The main drawback with this method was that the contrast between red and blue was not always easy to see through the microscope. The uncertainty in the front position was estimated to be 0.05 mm. Another concern was that for the wide tube,

the front would be axisymmetric or nonaxisymmetric instead of being flat. In these cases, the front position was measured at the leading edge. In order for this to work, the convecting front had to be given time (about half an hour) to completely form before measurements could be made.

### 2.3.2 Gatling Method

The gatling method allowed the front speed of all eight tubes to be measured simultaneously at a given angle. To obtain the front position, white paper was taped to the board. The board was then placed on the dexion and rotated to the proper angle, using the polar plot paper as before. The tubes were then mounted onto the board. The initial front positions were marked on the paper. Beside each mark was written the time from a stopwatch. For about 3 hours, at half hour intervals, the front positions were marked on the paper and the time was written on the paper beside the marks. When all the runs that could be obtained from the tubes were finished, the paper was removed from the board. A 30 cm ruler was used to measure the positions of the marks on the paper, and this data together with the times was used to calculate the front speeds.

This method allowed for only seven data points to be taken, and these positions had a much greater uncertainty than for the travelling microscope. However, since these measurements were taken over a much greater distance, the uncertainty in the front velocities was about the same as for the travelling microscope. Also, given the length of time taken for the runs, only two or three angles could be measured per day.

This method had several advantages over the travelling microscope method. Although it required more time to measure a particular angle, all eight tubes were measured simultaneously at that angle. Thus, overall the method was faster. It was much easier to see the front with the naked eye than it was through the microscope, so there were no difficulties locating the front. The error on the front position was estimated to be about 0.4 mm. This method also reduced the systematic errors due to possible nonuniform tube diameters by spreading the data taking out over a larger

length of tube.

### 2.3.3 Calculations

Once the positions and times were known for a front, this data was entered into a computer to be analyzed. The computer program used the numerical fitting routine *fit* from [12] to fit the data to a straight line using a least-squares fitting routine. A sample plot of this is found in Figure 2.2, and a plot of the resulting residuals is found in Figure 2.3. The sample plots use the data from the gatling method for straight upwards propagation in tube A.

Once the front speeds were calculated, it was necessary to determine the angles at which the front speeds in each tube were at their greatest. To do this, the gatling data was analyzed using the Levenberg-Marquardt method [12] to fit the front speed data to a third order polynomial. For the four large tubes, the data from 120° to 180° was used. For the four small tubes, the data from 0° to 90° was used. The fitted parameters were then used to calculate the maximum of the fit, thus giving an estimate of the maximum angle.

## 2.4 Error Analysis

There were a number of sources of error in this experiment. One of the most important was the triggering method. As stated previously, the amount of acid used to trigger the reaction was not very well controlled. This meant that the fronts all had different initial conditions. Previous work [3, 6] shows that the chemistry of the solution affects the front speed. By changing the amount of acid present initially, the initial chemical concentrations may have been slightly different. How great an effect this would play on the resulting fronts is unknown. If we assume that front speed is faster than acid diffusion, such an error would disappear over time. More important might be how the acid affects the indicator.

The Congo Red indicator may have been the cause of some serious problems. It was observed that after the solution had reacted, it remained blue for a brief period

Figure 2.2: Front Speed Calculation with Line of Best Fit
Front Speed is $(6.36 \pm 0.04) \times 10^{-3}$ mm/s

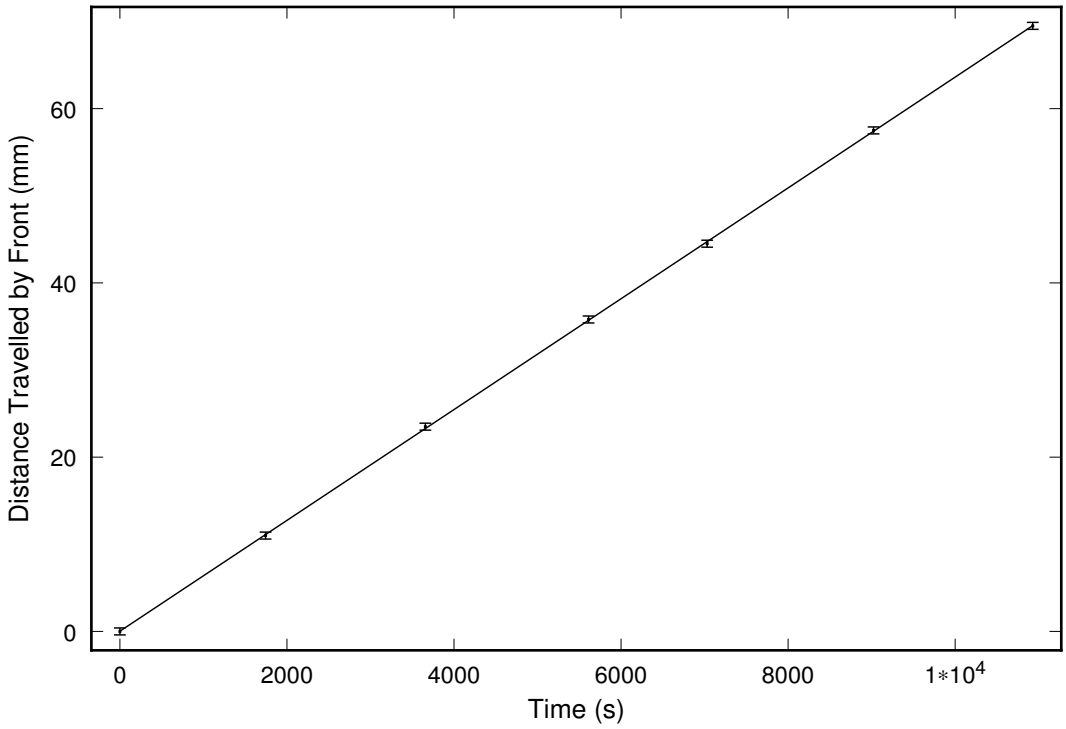


Figure 2.3: Front Speed Residuals

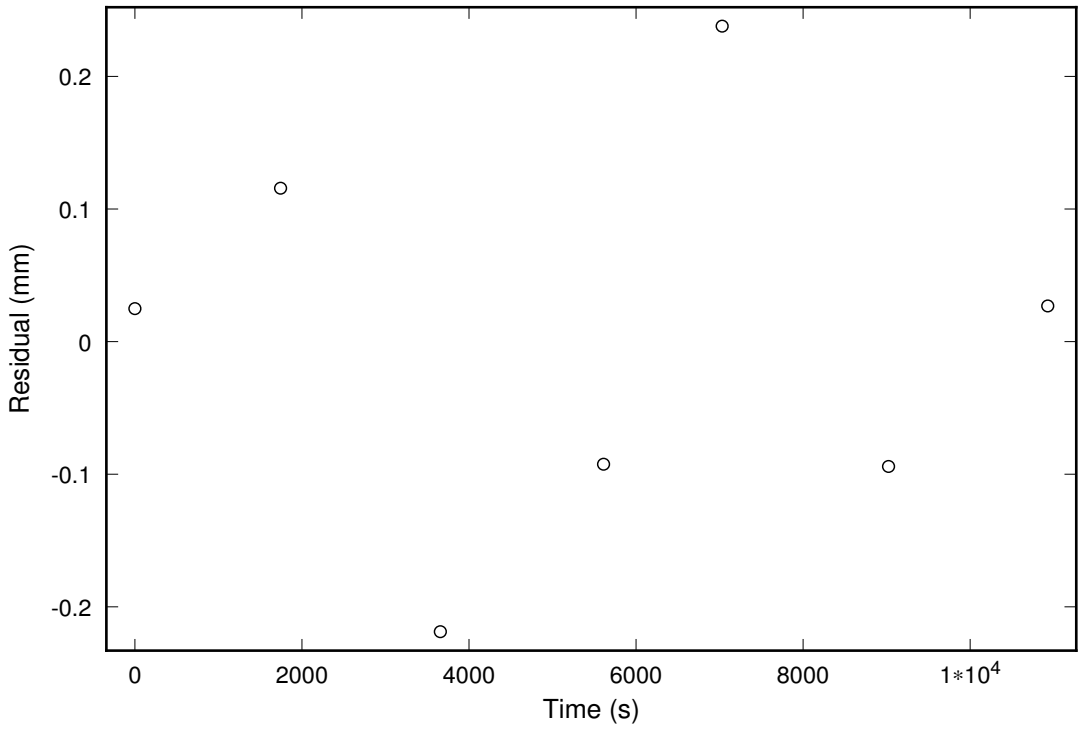

and then turned a dirty yellow colour. The source of this color change is not known. However, this change formed a front that mirrored the red-blue reaction front. In the yellow solution, globs of some sort of brown-black deposit formed. What this brown-black deposit was is unknown, although it is suspected that this material might be indicator that had reacted with the acid used to trigger the reaction. In the thicker tubes, these globs would sometimes fall under gravity down the tube. If the front was going downward, this brown-black deposit would sometimes catch up to and pass through the front. As it did so, the front would be smeared and the reacted and unreacted solution around the brown-black deposits would mix. This mixing would have the effect of increasing the front speed for the duration of the passage. Thus, any data taken during or after this brown-black deposit passage would be meaningless.

Another possible problem with the Congo Red dye is that over time it may break down and come out of solution. It was observed that if a sample of the solution is left exposed to air a residue forms on the walls of the jar. A sample of solution was left exposed for several weeks and as the residue built up the solution lost its red color, indicating that the residue was dye that had come out of solution. This was also observed in the stock solution. However, the stock did not begin to show signs of breaking down until several months after the experiments were completed.

A contaminant problem occurred during the travelling microscope measurement of the 2.05 mm tube. A sample of working solution was removed from the 2 litre flask and placed in an open glass jar for use. Initial use of this sample showed useful results. However, front speed measurements taken several days later were much larger than those previously observed. When angles were remeasured, the two front speeds differed by a factor of two. Evaporation of the solution may have changed the concentrations of the reactants, leading to the greater front speeds [3]. Dye residue was also observed in the jar. Either of these factors could have contributed to the unrepeatability of the front speed measurements. This problem did not occur for the gatling method, because a full jar of solution was needed to fill all eight tubes.

Another major source of error was the capillary tubes used. Differences in the inner diameter of a tube would result in the front having different speeds in different

parts of the tube, due to the front speed's dependence on tube diameter. The effect of any such nonuniformities would be magnified 3-fold, due to the cubic dependence of $S$ on the diameter.

To examine this possible source of error, the tubes were refilled, then set up in the straight up (180°) position using the gatling method. Over the course of two days five measurements of their front speeds were made. The measurements were timed to correspond with the locations in the tubes where measurements were usually made.

Table 2.2: Standard Deviations for the 8 Capillary Tubes.

| Tube | Diameter | Standard Deviation | Wall Type |
|---|---|---|---|
| A | $(2.781 \pm 0.006)$ mm | $24 \times 10^{-5}$ mm/s | Thick |
| B | $(2.559 \pm 0.006)$ mm | $7 \times 10^{-5}$ mm/s | Thick |
| C | $(2.417 \pm 0.006)$ mm | $29 \times 10^{-5}$ mm/s | Thin |
| D | $(2.249 \pm 0.006)$ mm | $9 \times 10^{-5}$ mm/s | Thick |
| E | $(2.05 \pm 0.01)$ mm | $12 \times 10^{-5}$ mm/s | Thick |
| F | $(1.90 \pm 0.02)$ mm | $6 \times 10^{-5}$ mm/s | Thick |
| G | $(1.80 \pm 0.01)$ mm | $7 \times 10^{-5}$ mm/s | Thick |
| H | $(1.53 \pm 0.01)$ mm | $4 \times 10^{-5}$ mm/s | Thick |

The standard deviations for the front speeds for this test are given in Table 2.4. These standard deviations were compared to the uncertainty from the fit program, which was $4 \times 10^{-5}$ mm/s. For the thin tubes (diameters below 2 mm), the standard deviations of the front speeds were of the same order of magnitude as the fit uncertainty. At most they were greater by a factor of two. Given that these standard deviations are on the order of the fit uncertainty, it was concluded that non-uniformities in these tubes was not a significant source of error. For three of the thicker tubes, B, D and E, the spread was not much greater. The remaining two tubes, A and C, were much worse. The non-uniformities were a serious source of systematic error in these tubes.

Given that these systematic errors are larger (sometimes much larger) than the uncertainties in the fits, these errors were used as the quoted uncertainties for the front speeds.

Another possible source of error was the room temperature. The temperature of

the solution in the tubes was not controlled, but varied with the temperature of the room. The room temperature ranged from 21°C to 23°C. In previous experiments, the capillary tubes were held at a constant temperature of $25.0 \pm 0.1°C$ [3, 6]. Tube C had thin walls, which would allow for greater heat gain/loss from the surroundings. Nagypàl *et. al.* [5] discovered that heat conduction through the capillary tube walls could play a role. However, that was for the exothermic chlorite-thiosulfate reaction, so the extent to which it their findings would apply to this case is unknown.

Finally, it was observed that when the tubes were rotated to a new angle, a sizable period of time was needed for the front to fully form. This time was on the order of half an hour or more for strongly convecting fronts. If measurements were taken too early, the resulting front speeds would be too large. Visual inspection of the data on a graph would show the first measurement to be significantly below a second fitted line formed by the remaining measurements alone. Once a systematically large "incorrect" initial measurement was identified it could be removed from the fit.

# Chapter 3

# Experimental Results

## 3.1 General Results

### 3.1.1 Front Observations

It was observed that for all of the capillary tubes, downward propagating fronts were flat and that each front moved at nearly the same speed. There was a tendency for front speeds to increase as the tube diameter increased, but this was insignificant within the uncertainties. The average downward speed was $(5.69 \pm 0.06) \times 10^{-3}$ mm/s.

Upwards propagating fronts showed evidence of convection, as expected. The onset of convection appeared to occur for tube diameters between 1.90 mm and 2.05 mm. Axisymmetric convection was seen in the two largest capillary tubes, A and B. The fronts in the other tubes appeared flat. However, increased front speed was observed in smaller tubes, indicating that convection was taking place. It is likely that in these cases the front curvature was so small that it was not readily apparent to the naked eye.

The value of $\delta$ used [9] predicted an onset diameter of $(1.49 \pm 0.07)$ mm. The experimental results do not agree with this prediction. In fact, the results give an $S_c$ of $(210 \pm 20)$. However, Carey had a reaction-diffusion speed of $(3.47 \pm 0.03) \times 10^{-3}$ mm/s [9], which does not agree with the results. This clearly shows that there was a difference in the chemistry of the solution used in this experiment and the solution

Carey used. Hence, the $\delta$ used in the calculations was most likely different from the actual $\delta$ of the solution and the predicted onset diameter is therefore incorrect.

Convection was also seen for inclined propagation. Very clear nonaxisymmetric fronts were observed in tubes A and B at angles 135° to 170°. Nonaxisymmetric fronts were present in some of the smaller tubes, but the distortion of the flat front was less pronounced and difficult to see.

While the main focus of this work was the iodate-arsenous acid front, there was another front to be observed. This was the interface between the blue reacted solution and the dirty yellow solution with unknown chemistry (see Section 2.4). The length of the blue solution was observed to remain constant at a given angle. As the angle changed, the length of the region would grow slightly as convection increased the speed of the front. It is possible that these different coloured regions formed a series of convective rolls along the length of the tube, and that this system of rolls moved at a uniform speed.

This second front exhibited the same behavior as the primary front. Axisymmetric and nonaxisymmetric convection at this front was observed in the two largest tubes, as was seen for the primary front. In addition to this, axisymmetric and nonaxisymmetric convection was also observed at this front in tubes C and D, even though such shapes were not observed at the primary front. It is likely that the density difference between the blue and yellow solutions was greater than the density difference between the red and blue solutions. This greater density difference would result in a more pronounced front. It is conceivable that this secondary front may have pushed forward a convectionless primary front in some instances.

As stated above, the size of the blue region remained constant, even if the blue-yellow front convected while the red-blue front appeared not to. Hence speeds of both fronts were the same, and only one needed to be measured. The speed of the red-blue front was measured, and the results are given in the next section.

### 3.1.2 Travelling Microscope Method

The travelling microscope method yielded results for capillary tubes A, E and G. The results are displayed in Figure 3.1. For tube A we observed a very large variation in front speed with angle, which indicated that convection was taking place. This convection is evident for all angles inclined away from straight down. The greater front speeds for angles past horizontal indicate that the two convection modes, axisymmetric and nonaxisymmetric, are at work. A numerical fit to this data places the maximum at $(159 \pm 16)^\circ$.

One curious feature of these results is a minimum in the front speed for horizontal propagation. Theory predicts that a horizontally propagating front should be convecting and thus the front speed should be greater than for straight down propagation. This is not the case. Repeated measurements verified that this minimum occurred consistently. The cause of this minimum is not known.

Tube G also showed a minimum front speed for a horizontal tilt. The tube was too small for upwards convection to take place, so this minima is the only source of variation in the front speed. It is possible that this minima is the result of some non-convective effect that was not taken into account in the theory.

The results for tube E are also worth mentioning, even though there are fewer data points available. We see some increase in front speeds away from straight down, which indicates that convection is occurring. This increase is much smaller in magnitude than that for tube A. Thus the convection is not as strong as it was in the larger tube. The angle of maximum front speed is $170^\circ \pm 50$. Again we see a minimum for horizontal propagation.

Theory predicts that for straight downwards propagation, the convectionless front speed will be a constant independent of capillary tube diameter. This is confirmed by the results of the experiment. The downward speeds for the three capillary tubes all agree to within the uncertainties. It is also predicted that without convection, the straight upwards propagation front speed will be the same as that for straight down, and that with convection the upwards speed will be greater than the downwards

Figure 3.1: Front Speeds as Function of Angle (Travelling Microscope Method)
Downwards Propagation Corresponds to 0°
Upwards Propagation Corresponds to 180°

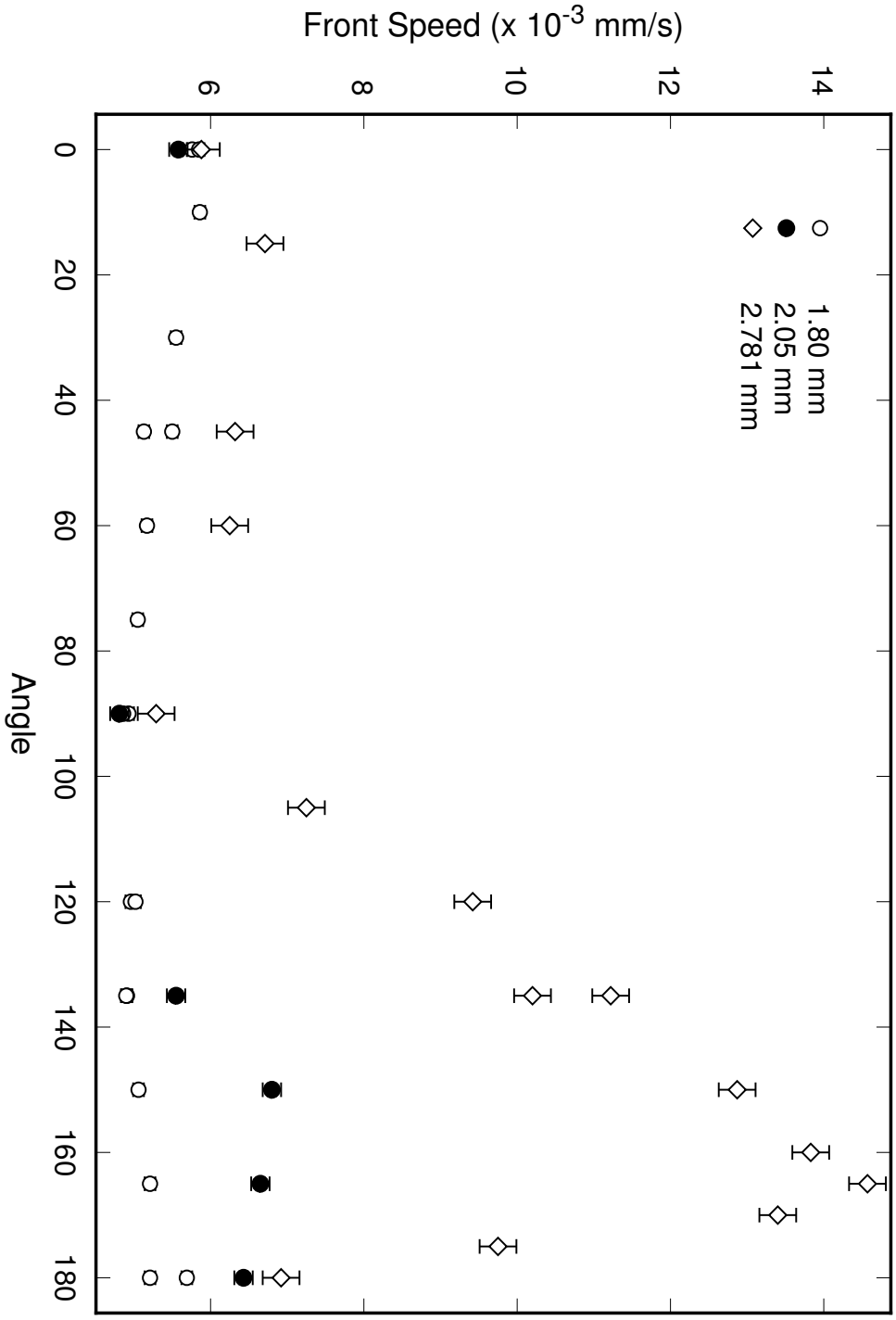

speeds. This is also verified.

### 3.1.3 Gatling Method

The gatling method yielded results for all eight tubes. The results are similar to what was found with the travelling microscope. The region between 135° and 180° was studied in detail, as before. However, less attention was paid to the region of angles below 90°. Figure 3.2 is a summary what was observed.

Figure 3.2 shows the same general features as Figure 3.1. The presence of convection is clearly indicated by the variation in front speeds for the capillary tubes as the angle changes. We see that as the tube thickness increases, so too does the front speed. Again we see the unexplained minimum for horizontal propagation. As well, the front speeds for the eight tubes are approximately the same for downwards propagation, as expected.

It is believed that no convection takes place for the three thinnest capillary tubes. If this is true, then the speeds for these fronts should be equal, since there is no convection to alter the front speeds. If we examine the results we see that there is much less variation in front speed for these three tubes than for the others. More importantly, the variation in front speed between these three tubes at any given angle is very small. For the most part, they are identical to within uncertainties. This confirms that convection is not taking place.

### 3.1.4 Comparison of Two Methods

The results for the two methods are compared in Figure 3.3. For the thin tube, G, we see that for the most part the two methods yield the same results. The agreement between the two methods is quite good, although the gatling method consistently yields slightly higher front speeds than the travelling microscope method.

The results for the thick tube, A, are somewhat different. The two methods yield the same qualitative results. For both methods there is a minimum at 90°. There is an increase in front speeds to both sides of this minimum. The results between

Figure 3.2: Front Speed as Function of Angle (Gatling Method)
Downwards Propagation Corresponds to 0°
Upwards Propagation Corresponds to 180°

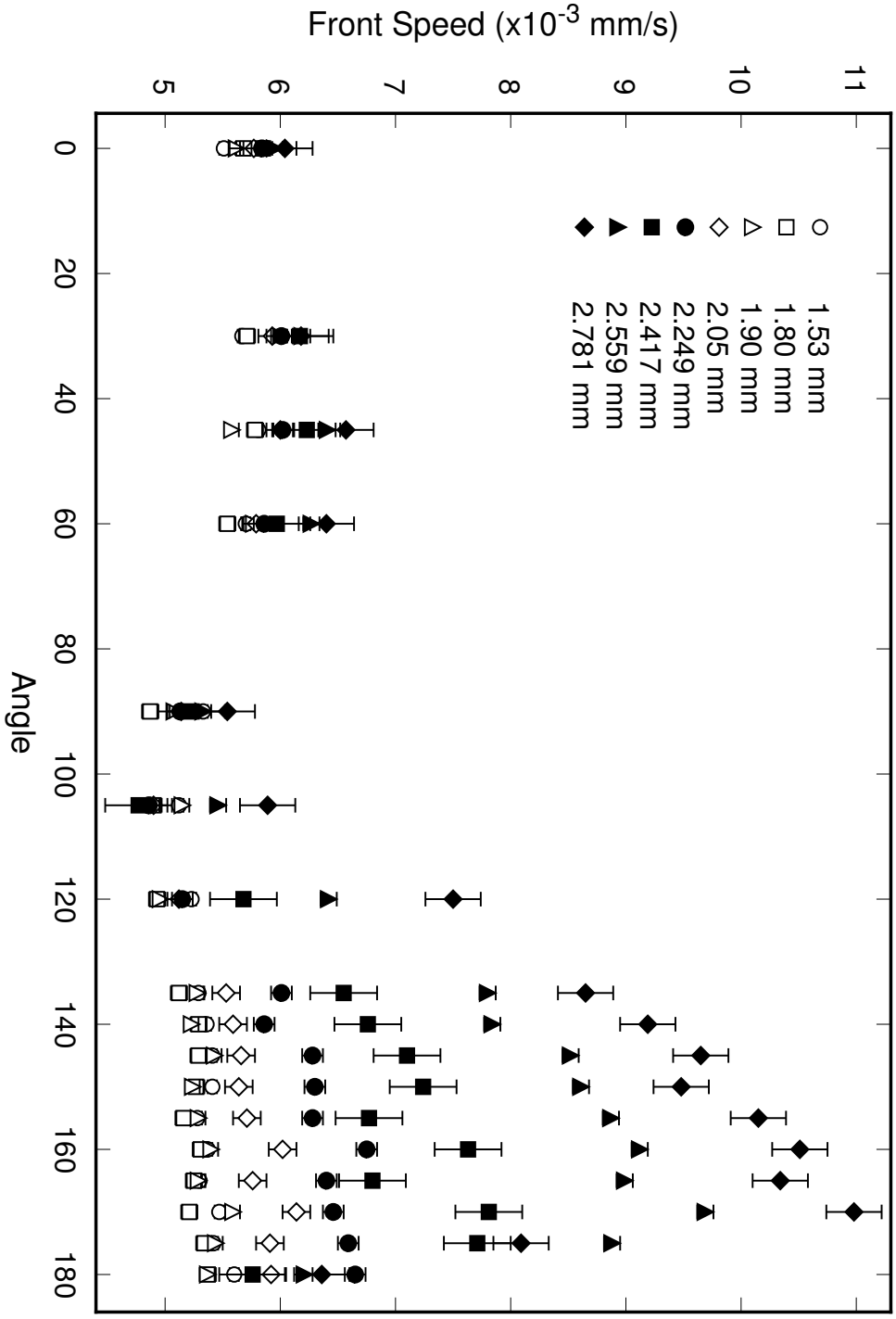

0° and 90° agree to within experimental error. However, between 90° and 180°, there is a considerable difference between the two methods. Qualitatively, the two methods agree. They both show a dramatic increase in front speed, and both have a maximum at approximately the same location. However, the front speeds for the travelling microscope method are much greater than those for the gatling method.

For the middle tube, E, we again see that the travelling microscope gives front speeds higher than the corresponding speeds for the gatling method. We also note that the qualitative results are different in that the maxima are different. However, there are fewer data points for the travelling microscope data, and this lack of data in the convecting region may be the cause of the observed differences.

One explanation for the differences between the two methods could be the length of capillary tube covered during a run. For the travelling microscope method, the front covers approximately 1.5 to 2.5 centimetres. The gatling method, since it requires a much longer run time, covers a distance ranging from from 5 cm to 15 cm. The length of this range varies greatly as the tube diameters and the angles change. Since the travelling microscope covers such a smaller range, it is much more susceptible to small variations in tube diameter. Such variations are averaged out over the length of the gatling method. This explanation does not explain the results for tube A, since the calculated error due to nonuniformities of $24 \times 10^{-5}$ mm/s is much smaller than the observed differences of $3 \times 10^{-3}$ mm/s.

Another possible explanation, particularly for tube A, could be that the fronts for the travelling microscope method were not given sufficient time to form and settle down. If the front has not settled by the time the first measurement is taken, the front speed calculated from the data is generally too high. This problem was detected and corrected for in the gatling method, but not in the travelling microscope method. However, this effect seems to be much too small to account for the discrepancy.

Figure 3.3: Plot of Front Speeds for Both Methods.
Downwards Propagation Corresponds to 0°
Upwards Propagation Corresponds to 180°

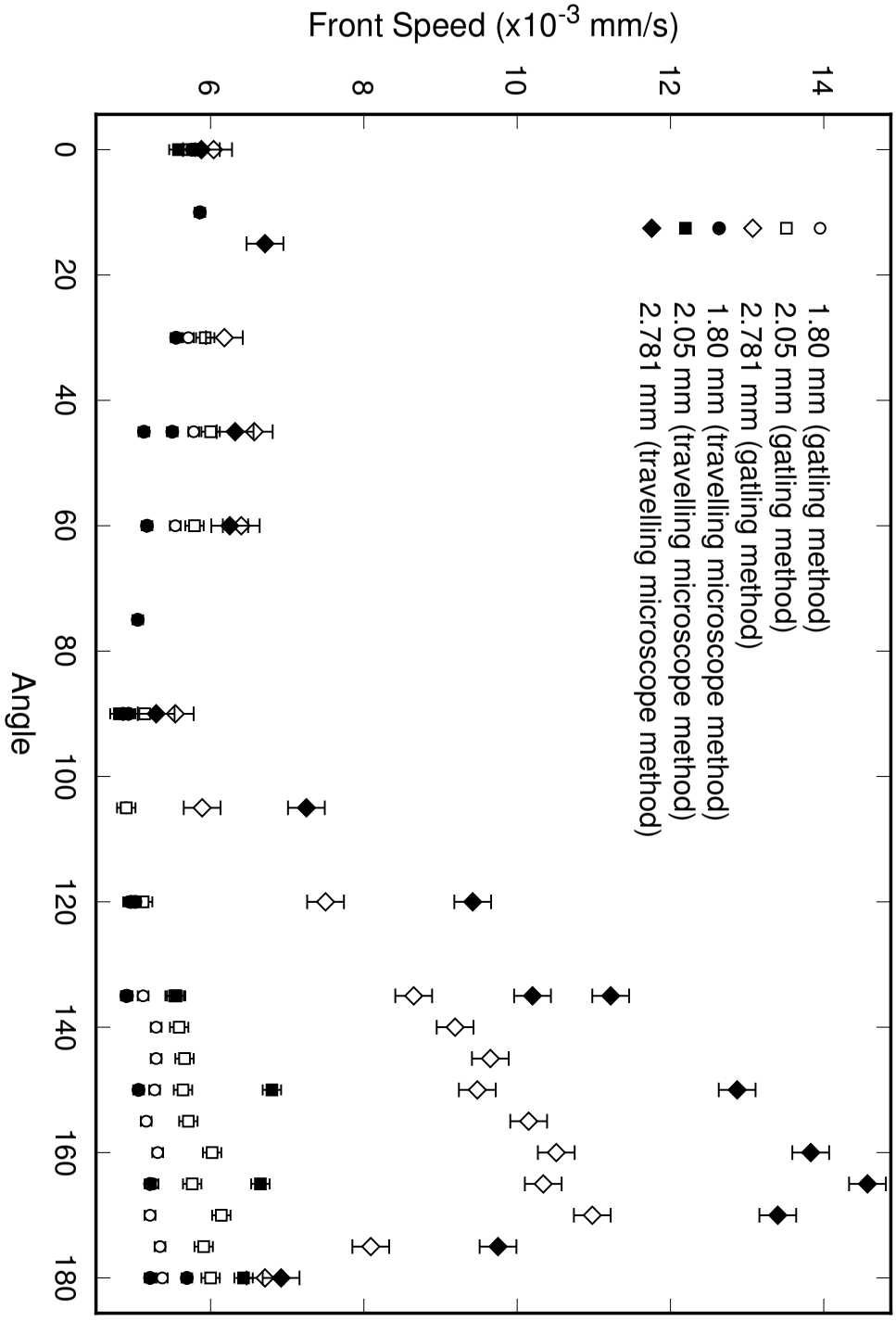

## 3.2 Front Speed as a Function of Tube Diameter

### 3.2.1 Upwards Propagation

Straight upwards propagation was studied with both methods. Theory predicts that for tubes with diameter below that needed for convection, the front speed should be constant. Once the diameter becomes large enough for convection, the front speeds should increase as a function of diameter.

The results of the experiment are shown in Figure 3.4. The closed circles correspond to the travelling microscope method, while the open circles correspond to the gatling method. For the gatling method, the small circles are the measured front speeds while the large circles are the average of the runs for the particular tube diameter. The error bars are the calculated standard deviations from the gatling method (see Section 2.4). In the cases where there is data for both methods, the results are in agreement to within the uncertainties.

The predicted theory is weakly borne out by the results. The three smallest tubes do have the smallest front speeds, and are approximately equal, but only to within two standard deviations. For larger diameters the front speeds do jump noticeably. The increase is not smooth, as one would expect. Tube D has a front speed much higher than expected, while the tube C has a front speed much lower than expected.

The major outlier in these results is tube C. This tube has a great deal of scatter, and at least one of the measured points lies in the expected region, even though the average does not. However, tube A also has a great deal of scatter, and its average is verified by the travelling microscope method data. Thus, scatter alone cannot be used to explain why tube C has a smaller than expected front speed. The reason may lie in the fact that tube C was the only thin-walled tube used. It was stated in Section 2.4 that the room temperature fluctuated over the course of the measurements. Tube C, with its thin wall, would thus be more susceptible to these temperature changes. These temperature changes could have affected rate of the reaction. Another possible reason for the large scatter may lie in the way the heat produced by the reaction diffused through the thin wall. Such effects were seen

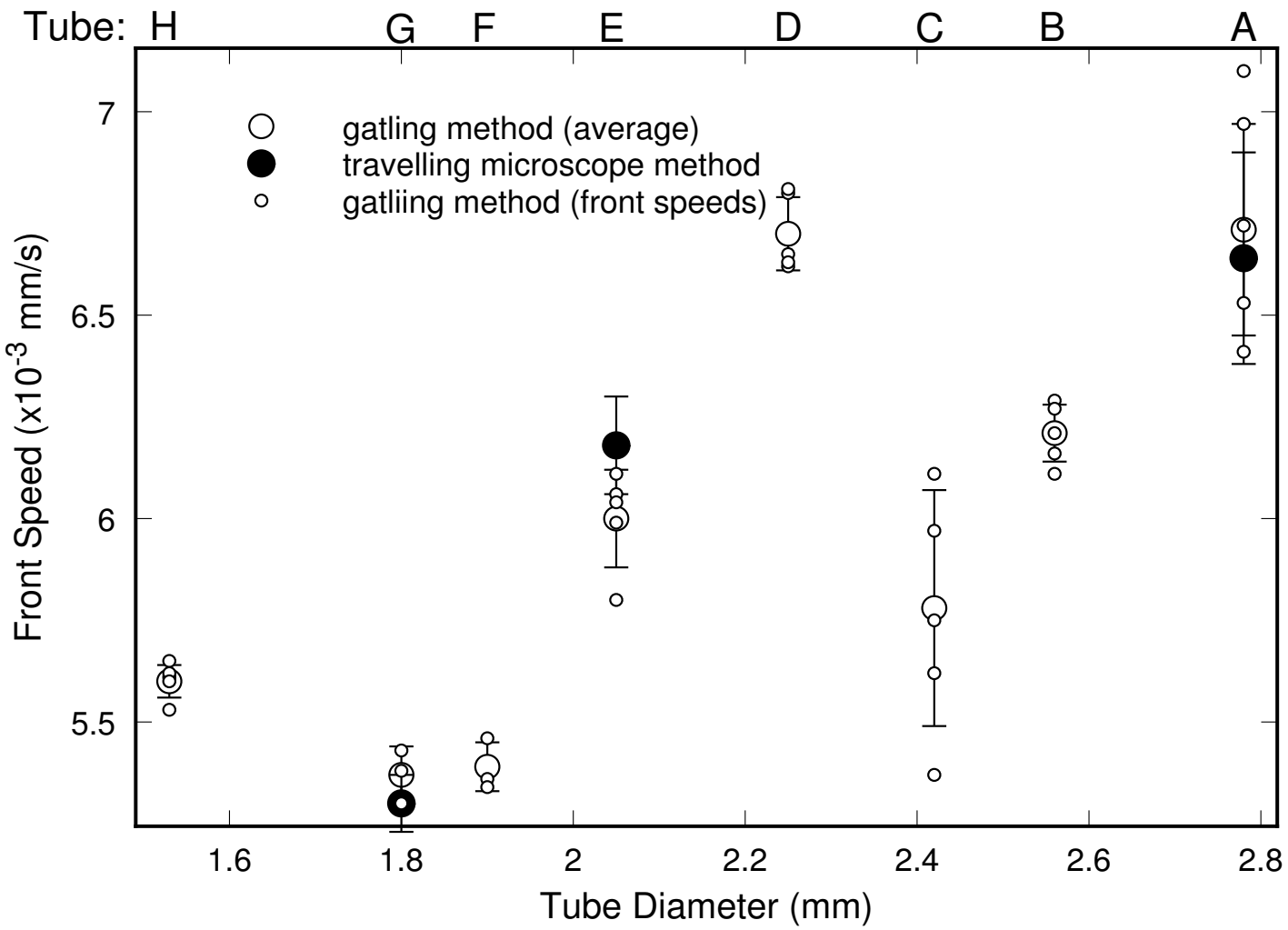


Figure 3.4: Plot of Front Speeds for Straight Upwards Propagation

in the highly exothermic chlorite-thiosulfate reaction [5], but the relevance of these observations to the iodate-arsenous acid reaction is unknown.

### 3.2.2 Downwards and Horizontal Propagation

The results, from the gatling method, for downwards and horizontal propagation are plotted in Figure 3.5. The closed circles denote downwards propagation while the open circles correspond to horizontal propagation.

The results for downward propagation are what was expected. To within the uncertainties, the front speeds are in agreement. The only possible exceptions are at the two extremes of tube size. Tube H has a front speed slightly lower than the others, while tube A has a front speed slightly higher than the others. These front speeds are roughly equal to or smaller than the front speeds for straight upwards propagation.

The results for horizontal propagation are more interesting. The theory predicts and previous experiments confirm that a horizontally propagating front will have a front speed greater than that of a front propagating downwards. This is clearly not the case. The horizontal front speeds, even with convection, are slower than the downwards front speeds. The difference is too great to be explained by experimental uncertainty. This phenomenon has not been seen before, and may be the result of some nonconvective effect caused by some aspect of the chemistry of the reaction, such as the added indicator.

The horizontal front speeds themselves are to a large degree constant. One would expect for pure convection that front speed would increase as the tube diameter increased. This expectation is only weakly borne out.

## 3.3 Maximum Front Speed as a Function of Angle

The angles at which the front speed was a maximum for the eight tubes were determined. Data from the gatling method was used. A summary of the results is plotted in Figure 3.6 and summarized in Table 3.1. It was found that the uncertainties in

Figure 3.5: Plot of Front Speeds for Horizontal and Straight Downwards Propagation

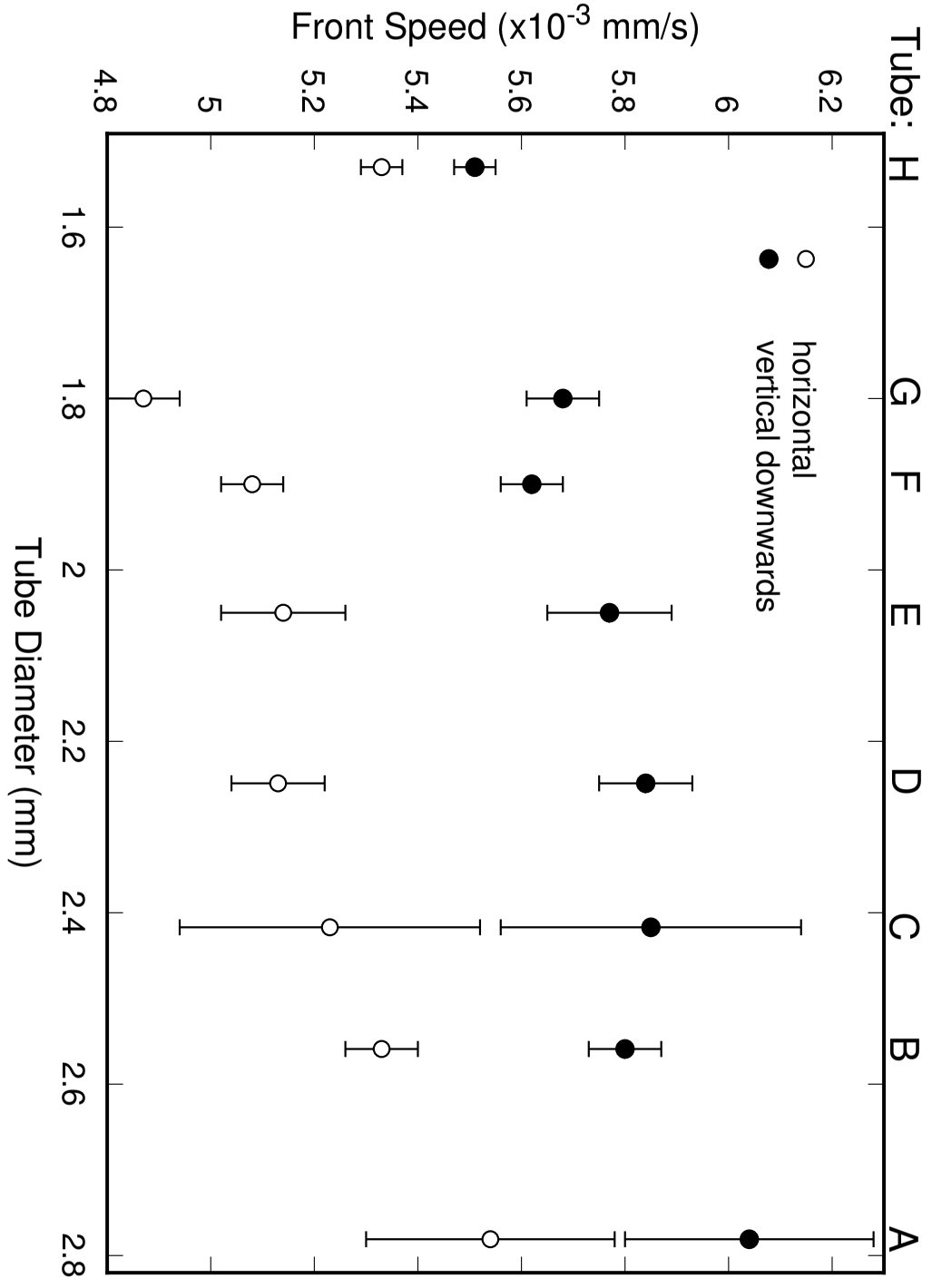

the fitted parameters was approximately 10%, and the quoted uncertainties in the calculated angles reflects this.

Table 3.1: Angle of Maximum Front Speed for Various Tube Diameters

| Tube | Diameter | Fitted Maximum |
|---|---|---|
| A | 2.781 mm | $(160 \pm 16)^\circ$ |
| B | 2.559 mm | $(161 \pm 16)^\circ$ |
| C | 2.417 mm | $(161 \pm 16)^\circ$ |
| D | 2.249 mm | $(180 \pm 18)^\circ$ |
| E | 2.05 mm | $(35 \pm 4)^\circ$ |
| F | 1.90 mm | $(29 \pm 3)^\circ$ |
| G | 1.80 mm | $(30 \pm 3)^\circ$ |
| H | 1.53 mm | $(49 \pm 5)^\circ$ |

For the four largest tubes, the angle of maximum front speed occurs in the region between 90° and 180°. For the smaller four tubes, the maximum angle between horizontal and straight upwards propagation is 180°. However, for these smaller tubes, the front speeds between 0° and 90° are comparable in size or larger than those between 90° and 180°. The maximum angle from this region for these four tubes is given in Table 3.3 and is plotted in Figure 3.3.

For the four largest tubes, there is a weak trend in which the angle of maximum front speed moves away from upwards vertical propagation (180°) as the tube diameter increases. The front in tube D moves fastest going straight up. The three larger tubes have their maxima at about 160°. There is a trend in which the angle decreases as the tube diameter increases, but this is negligible when compared to the estimated uncertainties. There is no such trend in the four smallest tubes.

One possible explanation for these results is the horizontal minimum. As the tube diameter decreases, this minimum has more of an effect. For the smaller tubes, in which there should be no convection, the effect of this minimum is to lower the horizontal and close to horizontal front speeds. This lowering leads to an apparent maximum where none should be. The minimum also counters the effects of convection in thin convecting tubes such as tube D. In these tubes, the maxima was lowered to such an extent that it no longer existed.

Figure 3.6: Plot of Maximum Front Speed Angle as a Function of Tube Diameter
Downwards Propagation Corresponds to 0°
Upwards Propagation Corresponds to 180°

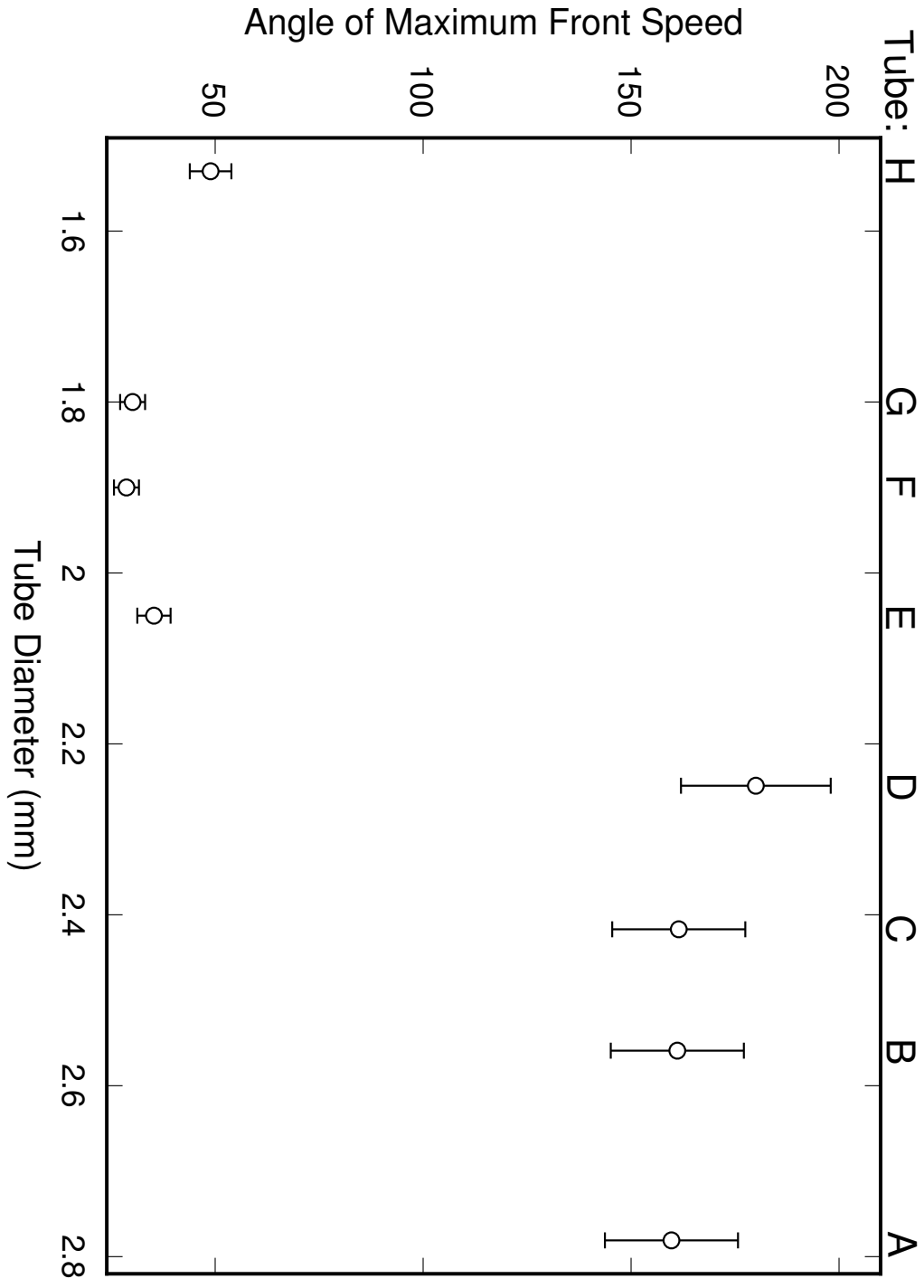

As a comparison between the gatling and travelling microscope methods, the angle of maximum front speed for capillary tube A was computed with data from the travelling microscope method. The calculated maximum was $(159 \pm 16)^\circ$, which is essentially the same as the result from the gatling method.

# Chapter 4

# Conclusions

Convection in the iodate-arsenous acid reaction was clearly observed. The onset of convection for upwards propagation occurred between 1.90 mm and 2.05 mm. This does not agree with the predicted onset value. However, due to the fact that the value of $\delta$ was taken from a reference instead of being measured, the prediction is probably not valid. Axisymmetric and nonaxisymmetric modes of convection were observed in some of the convecting tubes, while convection in other tubes had to be inferred from increases in front speed. It was found that in general, front speed at a given angle increased as a function of diameter. As well, front speed also changed as a function of angle. In the convecting tubes, the angle of maximum front speed was about 160°. The pure reaction-diffusion front speed was found to be $(5.69 \pm 0.06) \times 10^{-3}$ mm/s.

In addition to the observed convection, a second phenomenon was seen, in which the front speed was retarded for horizontal propagation. Such an effect was not predicted by theory, nor has it been seen in previous experiments. This effect appeared to compete with convection. As a result, some of the observations were not as expected. For example, non-convecting tubes showed variations in front speed and convecting tubes had front speeds that were lowered. This minimum affected the front speeds at inclinations away from the horizontal as well. As a result, the results cannot be compared to the existing model. This effect requires further study.

The chemistry of the iodate-arsenous acid mixture used raises some question. The use of a chemical indicator is believed to have resulted in some unexpected problems.

Burnt indicator is believed to be the source of brown-black deposits that interfered with some of the runs. It is also believed to be the cause of the blue-yellow front that appeared behind the primary front. The chemistry of the yellow solution was not known, although the more visible convection at this front indicated that the density difference at this front is greater than the difference at the primary front. The presence of the indicator may also have lead to the horizontal retardation of front speed, by influencing the chemistry in some way.

## 4.1 Suggestions for Future Work

There are several avenues in which further study is required. Clearly, more work is needed in studying the relation between tube inclination and front speed. While general trends were found in this study, more work must be done to eliminate the large scatter that was found. Such work might incorporate the use of temperature controlled capillary tubes with more uniform inner diameters.

The effect of external temperature might also be a topic of future study. The significant deviation between the results for the thin tube and the results for the thick tubes indicates that external temperatures are important.

A third topic for study is the observed minimum front speed for horizontal propagation. All of the previous studies, both theoretical and experimental, indicate that horizontal propagating front speeds should be greater than downwards propagating front speeds. The opposite was found in this study, and more work is required to determine what was different in this study.

Finally, the particular iodate-arsenous acid solution used could be studied. A number of previously unreported phenomenon, such as the second front and strange deposits, need to be explained. Other indicators could be tried instead of Congo Red. Different concentrations and pH are another avenue to explore.

# References


[1] Desiderio A. Vasquez, Joseph W. Wilder and Boyd F. Edwards, Phys. Fluids A, **4**, 2410-2414, 1992.

[2] Boyd F. Edwards, Joseph W. Wilder, and Kenneth Showalter, Physical Review A, **43**, 749-760, 1991.

[3] John A. Pojman, Irving R. Epstein, Terence J. McManus and Kenneth Showalter, J. Chem. Phys., **95**, 1299-1306, 1991.

[4] D. A. Vasquez, J. M. Littley, J. W. Wilder and B. F. Edwards, Physical Review E, **50**, 280-284, 1994.

[5] István Nagypál, Grörgy Bazsa, and Irving R. Epstein, J. Am. Chem. Soc., **108**, 3635-3640, 1986.

[6] Jonathan Masere, Desiderio A. Vasquez, Boyd F. Edwards, Joseph W. Wilder and Kenneth Showalter, J. Phys. Chem., **98**, 6505-6508, 1994.

[7] Joseph W. Wilder, Boyd F. Edwards, Desiderio A. Vasquez and Gregory I. Sivashinsky, Physica D, **73**, 217-226, 1994.

[8] Desiderio A. Vasquez, Joseph W. Wilder and Boyd F. Edwards, J. Chem. Phys, **98**, 2138-2143, 1993.

[9] Michael R. Carey, Stephen W. Morris and Paul R. Kolodner, Physical Review E, **53**, 6012-6015, 1996.

[10] D. Vasquez, private correspondence.

[11] P. Kolodner, private correspondence.

[12] William H. Press, Saul A. Teukolsky, William T. Vetterling and Brian P. Flannery, *Numerical Recipes in C: The Art of Scientific Computing*, Cambridge University Press, Cambridge, 1992.